

1 **Intranasal Immunization with a Proteosome-Adjuvanted SARS-CoV2 Spike**

2 **Protein-Based Vaccine is Immunogenic and Efficacious in Mice & Hamsters**

3

4

5 Felicity C. Stark¹, Bassel Akache^{*1}, Lise Deschatelets¹, Anh Tran¹, Matthew Stuitable¹, Yves Durocher¹,
6 Michael J. McCluskie¹, Gerard Agbayani¹, Renu Dudani¹, Blair A. Harrison¹, Tyler M. Renner¹, Shawn R.
7 Makinen¹, Jegarubee Bavananthasivam¹, Diana Duque¹, Martin Gagne², Joseph Zimmermann², C. David
8 Zarley^{3,4}, Terrence R. Cochrane^{3,5} and Martin Handfield³.

9

10 Affiliations:

11 ¹ National Research Council Canada, Human Health Therapeutics, 1200 Montreal Road, Ottawa, Ontario,
12 Canada, K1A 0R6.

13 ² Inspirevax Inc., 46 rue de Saint-Tropez, Kirkland, Quebec, Canada, H9J 2K6.

14 ³ Oragenics, Inc., 13700 Progress Blvd, Alachua, Florida, USA, 32608.

15 ⁴ CDZarley LLC., 133 Butternut Dr, Pottstown, Pennsylvania, USA, 19464.

16 ⁵ BrevisRefero Corporation, 295 Alliance Road Suite 1B/C Milton, Ontario, Canada, L9T 2X7.

17 ^{*}Corresponding Author

18

19 **Abstract**

20 With the persistence of the SARS-CoV-2 pandemic and the emergence of novel variants, the development
21 of novel vaccine formulations with enhanced immunogenicity profiles could help reduce disease burden
22 in the future. Intranasally delivered vaccines offer a new modality to prevent SARS-CoV-2 infections
23 through the induction of protective immune responses at the mucosal surface where viral entry occurs.
24 Herein, we evaluated a novel protein subunit vaccine formulation containing a resistin-trimerized
25 prefusion Spike antigen (SmT1v3) and a proteosome-based mucosal adjuvant (BDX301) formulated to
26 enable intranasal immunization. In mice, the formulation induced robust antigen-specific IgG and IgA
27 titers, in the blood and lungs, respectively. In addition, the formulations were highly efficacious in a
28 hamster challenge model, reducing viral load and body weight loss. In both models, the serum antibodies
29 had strong neutralizing activity, preventing the cellular binding of the viral Spike protein based on the
30 ancestral reference strain, the Beta (B.1.351) and Delta (B.1.617.2) variants of concern. As such, this
31 intranasal vaccine formulation warrants further development as a novel SARS-CoV-2 vaccine.

32

33

34

35

36

37

38

39

40

41

42 **Keywords:** COVID-19; SARS-CoV-2; Spike glycoprotein; BDX301; Vaccine; Adjuvant; SmT1; Mucosal; IgA;
43 NT-CoV2-1

44 **Introduction**

45 The etiological agent of the COVID-19 pandemic, SARS-CoV-2, has proven to be highly virulent and
46 adaptable. Despite the development and deployment of multiple relatively safe and efficacious vaccines
47 worldwide, the emergence of novel viral variants with decreased sensitivity to vaccine-induced immune
48 responses has caused the pandemic to persist and still present a major challenge to human health ¹⁻³.

49 In the initial response to the COVID-19 pandemic, vaccine developers were able to produce efficacious
50 vaccines targeting SARS-CoV-2 with unprecedented speed by utilizing several established and novel
51 vaccine platforms. Inactivated virus vaccines (e.g. Sinopharm's BBIBP-CorV and Sinovac's CoronaVac), as
52 well as mRNA- (e.g. Pfizer-BioNTech's Comirnaty® and Moderna's Spikevax®) and viral vector-based
53 vaccines (e.g. Oxford-AstraZeneca's Vaxzevria® and Janssen/Johnson & Johnson's Ad26.COV2.S) quickly
54 advanced through clinical trials to regulatory approval due to their strong immunogenicity/efficacy, but
55 also in part to their relatively rapid manufacturing processes ⁴⁻⁶. As such, they were the first wave of
56 SARS-CoV-2 vaccines to become widely available in many parts of the world including China, North
57 America and Europe. However, questions remain regarding their efficacy and safety in the long term.
58 Although rare in frequency, severe cases of anaphylaxis, myocarditis and/or thrombocytopenia have been
59 linked specifically to the mRNA and viral vector vaccine platforms⁷⁻⁹. With the emergence of novel COVID-
60 19 variants of concern capable of partially evading the protection induced by the currently approved
61 vaccines ^{1-3,10}, the development of novel vaccines with improved safety and efficacy profiles could reduce
62 the impact of SARS-CoV-2 and its variants in the future.

63 SARS-CoV-2 is an airborne pathogen that enters the body primarily through the upper respiratory tract
64 (URT; nose and mouth). The URT is likely the initial location of infectivity as it contains a much greater
65 concentration of ACE2 receptors than the lower respiratory tract ^{11Error! Reference source not found.}. Immune
66 responses initiated in these mucosal sites often involve mucosa-associated lymphoid tissues (MALT),

67 which are a compartmentalized immunological system that functions independently from the
68 systemic immune apparatus¹². This localized system includes epithelial cells that take up antigen,
69 which is subsequently shuttled to or captured by antigen presenting cells (APCs, i.e. dendritic cells,
70 macrophages) and presented to CD4⁺/CD8⁺ T-cells all located within the mucosal inductive site¹³.
71 Intranasal vaccines have the potential to induce systemic immune responses as with parenteral vaccines,
72 but can also generate robust broadly protective mucosal immune responses based on secretory IgA
73 antibodies and tissue-resident T cells at the mucosal surface of the respiratory tract at the site of viral
74 entry potentially limiting infection before it becomes established¹⁴. This in turn could lead to reduced
75 transmission of SARS-CoV-2 in vaccinated populations relative to vaccines delivered parenterally. In
76 addition, due to the non-invasive nature of vaccine administration, it may increase vaccine uptake in the
77 wider population.

78 Mucosal adjuvants are considered essential in activating mucosal immunity to overcome the natural
79 tolerance to antigens encountered in this compartment¹⁵. A number of adjuvants have
80 demonstrated an ability to potentiate adaptive and innate immunity when administered on a
81 mucosal surface¹⁶⁻¹⁸. BDX301 is a Proteosome-based adjuvant composed of porin proteins and
82 lipooligosaccharides from *Neisseria meningitidis*. Proteosomes are a family of mucosal adjuvants
83 derived from the outer membranes of Gram-negative pathogenic bacteria and have shown strong
84 activity when delivered intranasally, inducing high levels of antigen-specific IgA within the respiratory
85 tract¹⁹⁻²¹. In fact, influenza vaccines containing these types of adjuvants have been shown to be safe and
86 effective in human clinical trials^{22,23}. Previously, a nasal vaccine comprised of a SARS-CoV-1 recombinant
87 Spike protein with another Proteosome based adjuvant, Protollin, elicited similar serum neutralizing
88 antibody levels as an aluminum hydroxide-adjuvanted formulation containing the same antigen
89 administered intramuscularly, but had significantly lower and undetectable lung SARS-CoV-1 viral titres at
90 3 days post-challenge, compared to aluminum hydroxide, in a mouse model²⁴.

91 With the persistence of SARS-CoV-2, vaccines based on different technologies and routes of
92 administration warrant investigation. We have previously demonstrated the strong immunogenicity of a
93 resistin-trimerized SARS-CoV-2 Spike antigen, referred to as SmT1²⁵. Intramuscular administration of
94 adjuvanted vaccine formulations of SmT1 induced robust immune responses that were strongly protective
95 in a hamster challenge model. Herein, we evaluated the immunogenicity and efficacy of intranasal vaccine
96 formulations based on a FLAG and histidine tag-less version of SmT1 (i.e. SmT1v3) and the mucosal
97 adjuvant BDX301 in preclinical models. Overall, we demonstrate that intranasal administration of the
98 vaccine formulations induces high levels of antigen-specific IgG and IgA in mice and is efficacious in a
99 hamster challenge model, preventing body weight loss and eliminating viral load in lungs/nasal turbinates.

100 **Results**

101 *IgG antibody response in immunized mice*

102 BALB/c mice (n=10/group) were immunized by intranasal instillation with vaccine formulations consisting
103 of SmT1v3 alone or adjuvanted with BDx301 on Days 0 and 21. SmT1v3 based on the ancestral reference
104 strain originally identified in Wuhan was used for all vaccine formulations in this study. Controls included
105 mice injected with the vaccine vehicle, phosphate-buffered saline (PBS), or SmT1v3 adjuvanted with
106 aluminum phosphate (AdjuPhos™). Aluminum phosphate is a conventional vaccine adjuvant found in a
107 number of approved vaccines and is a potent inducer of antigen-specific antibody responses^{26,27}. SmT1v3-
108 AdjuPhos™ formulations were delivered intramuscularly²⁸. To assess the ability of the vaccine
109 formulations to induce systemic immune responses following one or two vaccine doses, serum samples
110 were taken on Days 21 and 35, respectively.

111 Following a single vaccine dose, SmT1v3 adjuvanted with BDx301 or aluminum phosphate induced
112 statistically similar anti-Spike IgG Geomean Titers (GMT) of 5,288 and 7,091 ($p>0.05$), respectively, in the
113 sera of immunized mice (Fig. 1A). These levels were significantly greater than those observed in animals
114 immunized with antigen alone or vehicle control ($p<0.0001$). Antigen-specific antibody titers were
115 increased >20-fold in the sera of mice following administration of a second vaccine dose of SmT1v3
116 adjuvanted with BDx301 or aluminum phosphate, with measured GMTs of 392,690 and 163,003,
117 respectively ($p>0.05$; Fig. 1B). Again, they were significantly greater than both control groups ($p<0.0001$),
118 which still showed low or non-detectable antibody titers.

119 *Neutralization response in immunized mice*

120 While the induction of anti-Spike IgG antibodies is currently thought to be a strong predictor of vaccine
121 efficacy against COVID-19²⁹, the functionality of these antibodies as measured by their ability to prevent
122 viral Spike binding to the cells and prevent infection is especially important. Using a surrogate cell-based
123 neutralization assay previously shown to have a strong correlation to responses obtained with viral-based

124 SARS-CoV-2 assays²⁸, we evaluated the neutralization activity of the immunized mouse serum against the
125 ancestral reference strain and Beta variant of concern (VOC). The assay measures the ability of serum
126 antibodies to prevent binding of Spike protein to the ACE2 receptor on the surface of VERO E6 cells.
127 Mutations within the Spike protein from the Beta VOC, have made it especially resistant to neutralization
128 by antibodies induced by the reference strain³⁰. SmT1v3-BDX301 vaccine formulations induced strong
129 neutralizing activity against both the ancestral and Beta SARS-CoV2 Spike proteins, which was significantly
130 higher than with antigen alone (Fig. 2; $p < 0.0001$). Additionally, the BDX301-adjuvanted formulation
131 induced significantly greater neutralization than that observed with the SmT1v3-aluminum phosphate
132 formulation against the Beta variant (71 vs. 35%; $p < 0.05$), while neutralization was statistically similar
133 against the Spike from the ancestral reference strain (93 vs. 80%; $p > 0.05$).

134 *IgA antibody response in immunized mice*

135 As enhancement of local IgA responses in the mucosal compartment is typically one of the main
136 advantages of mucosal proteosome-adjuvanted vaccine formulations, antigen-specific IgA titers were also
137 assessed in the bronchoalveolar lavage (BAL) fluid and serum of mice collected on Day 35. Only SmT1v3-
138 BDX301 immunized mice showed detectable anti-SmT1v3 IgA titers, as titers in mice immunized with
139 antigen alone or SmT1v3-aluminum phosphate were below the assay's limit of detection (Fig. 3). In both
140 the BAL fluid and serum, IgA titers were significantly higher than the control groups with a GMT of 1,000
141 and 5,074 in the BAL and serum, respectively ($p < 0.0001$). Interestingly, the anti-SmT1v3 IgG/IgA ratio was
142 ~25-fold lower in the BAL vs. serum ($p < 0.01$; Fig. 3D), indicating that the antigen-specific IgA detected in
143 the BAL was not simply due to cross-contamination with blood or leakage of blood through the mucosal
144 epithelium. Having established the immunogenicity of a vaccine formulation based on BDX301 and
145 SmT1v3 in mice, we next sought to evaluate its efficacy against a live SARS-CoV-2 challenge in hamsters.

146

147 *IgG antibody response in immunized hamsters*

148 Golden Syrian hamsters are a widely accepted model to evaluate vaccines against SARS-CoV-2, due to
149 their susceptibility to infection as well as the manifestation of similar disease pathology in the lungs to
150 that seen in COVID-19 patients with pneumonia^{31,32}. Golden Syrian hamsters were immunized intranasally
151 twice on Days 0 and 21 with BDX301 alone, or in combination with 5 or 15 µg of SmT1v3. A negative
152 control group dosed with PBS alone was also included. We first sought to measure the immunogenicity of
153 the vaccine formulations in hamsters. Serum samples were collected on Days 20 and 35 to assess anti-
154 SmT1v3 IgG titers. As expected, both doses of SmT1v3-BDX301 induced high levels of antigen-specific IgG
155 titers that were significantly higher than seen in the antigen alone or vehicle control groups at either
156 timepoint (Fig. 4; $p < 0.0001$). At Day 20, significantly greater GMTs of anti-SmT1v3 IgG were induced by
157 BDX301 formulations containing 15 µg vs. 5 µg antigen (2,766 vs. 718; $p < 0.001$; Fig. 4A). By Day 35, 14
158 days post the second immunization, the GMT titers were still higher with 15 µg vs. 5 µg, but they did not
159 reach a level of statistical significance (19,492 vs. 8,510; $p > 0.05$; Fig. 4B).

160 *Neutralization response in immunized hamsters*

161 As with mice, the neutralization activity of the immunized hamster serum was assessed, but in addition
162 to the ancestral reference strain and Beta VOC, the Spike protein from the Delta VOC was also included.
163 The BDX301 formulations with either 5 µg or 15 µg antigen induced strong neutralization activity to the 3
164 different Spike variants. The strongest neutralization activity was seen against the ancestral reference
165 strain, with BDX301 with 5 or 15 µg of SmT1v3 inducing an average of 55 and 71% neutralization,
166 respectively ($p < 0.0001$ vs. vehicle or adjuvant alone groups; Fig. 5A). While neutralization activity against
167 the Beta variant was detected in many animals immunized with BDX301-SmT1v3, it did not reach a level
168 of statistical significance when compared to the control groups (Fig. 5B). Neutralization activity against
169 the Delta variant was quite strong, with an average of 39 and 52% neutralization measured in the sera of
170 animals immunized with BDX301 with 5 and 15 µg of SmT1v3, respectively. ($p < 0.05$ vs. control groups;
171 Fig. 5C). A plaque reduction neutralization test was also conducted to test the ability of the serum samples

172 to block infection of VERO E6 cells by live SARS-CoV-2 (ancestral reference strain). Either antigen dose
173 combined with BDx301 induced significantly greater neutralization compared to vehicle or adjuvant alone
174 ($p < 0.0001$) (Fig. 5D).

175

176 *SARS-CoV-2 viral challenge of immunized hamsters*

177 On Day 42, hamsters were challenged with 1×10^5 PFU of SARS-CoV-2 (ancestral reference strain) and
178 monitored daily for body weight change post-challenge. At 5 days post-challenge, the BDx301 adjuvant
179 alone and PBS vehicle control groups lost ~9 and 11% of their body weight, respectively, with no significant
180 difference between the two (Fig. 6). Hamsters immunized with either 5 or 15 μ g of SmT1v3 were protected
181 from body weight loss over the course of the study, demonstrating significantly less body weight loss than
182 both control groups ($p < 0.0001$; Fig. 6A). On Day 47, hamsters were euthanized and viral titers were
183 quantified in lung and nasal turbinates by plaque assay. While viral load was high in control animals
184 immunized with PBS or adjuvant alone, no viral titers were detected in tissues of animals immunized with
185 BDx301 combined with 5 or 15 μ g of SmT1v3 (Fig. 6B & 6C). Importantly, as the adjuvant alone group did
186 not protect hamsters from body weight loss or viral replication, we can deduce that the observed
187 protection in this study was largely mediated by antigen-specific responses and not innate immune
188 activation.

189 Discussion

190 The purpose of this study was to first conduct an immunogenicity comparison of the intranasal adjuvant
191 BDX301 using the conventional intramuscular adjuvant aluminum phosphate (AdjuPhos™) as a
192 benchmark in mice with the ancestral Wuhan strain recombinant Spike protein SmT1v3, a FLAG and
193 histidine tag-less version of SmT1, which was previously described elsewhere²⁵. In the second part of our
194 study, we assessed the inhibition of virus replication in hamsters immunized with SmT1v3 formulated with
195 BDX301, hereafter referred to as NT-CoV2-1. Two intranasal doses of NT-CoV2-1 elicit strong serum IgG
196 binding and neutralization responses to the ancestral Wuhan strain that are comparable to those seen
197 following intramuscular dosing with SmT1v3 formulated with aluminum phosphate. Neutralization
198 responses induced by NT-CoV2-1 to the Beta (B.1.351) variant were significantly higher than observed
199 with the aluminum phosphate-adjuvanted formulation ($p < 0.05$). No measurable responses were seen
200 with the antigen alone controls.

201 A key differentiating feature of intranasal administration of NT-CoV2-1 is the IgA response seen in BAL
202 and serum in mice, which was not seen in mice following intramuscular administration of SmT1v3
203 formulated with aluminum phosphate or intranasal immunization with SmT1v3 alone. These results are
204 consistent with other animal studies using intranasally administered recombinant SARS Spike protein²⁴
205 and vector-expressed SARS-CoV-2 Spike protein constructs³³ and suggest that intranasal immunization
206 may be necessary to induce BAL IgA antibodies.

207 In hamsters, NT-CoV2-1 induced high levels of antigen-specific IgG titers and neutralization activity to the
208 ancestral Wuhan strain, as well as neutralization activity against the Beta (B.1.351) and Delta (B1.617.2)
209 variants, though at reduced potency than for Wuhan. Interestingly, the Delta variant appeared more
210 susceptible than the Beta variant to neutralization by antisera induced by the ancestral Wuhan strain, as
211 has been reported elsewhere in the literature³⁴. The intranasal challenge of hamsters receiving two

212 intranasal doses of NT-CoV2-1 confirmed the functional activity of the immune response, as hamsters
213 maintained weight and showed no measurable virus titer in lungs or nasal turbinates. Control hamsters
214 showed significant weight loss and residual virus in both tissues. These results are consistent with the
215 benchmark set with other COVID-19 vaccine candidates that have proceeded to clinical trial.

216 Intramuscularly administered COVID-19 vaccines have proven highly effective in preventing COVID-19
217 symptomatic disease, hospitalization and death. However, recent experience with these vaccines suggest
218 they may not be as effective in preventing virus transmission, particularly with newly emerging variants
219 such as Delta and Omicron³⁵. It has been posited that induction of local immunity in the nasal-pharyngeal
220 cavity by intranasal vaccine administration could reduce viral shedding and transmission, which has been
221 supported by recent studies in hamsters and rhesus macaques^{36,37}. Hence there is growing interest in
222 developing an intranasal COVID-19 vaccine with potential to reduce virus transmission more effectively³⁸.

223 **Conclusion**

224 NT-CoV2-1 is composed of a recombinantly expressed ancestral Wuhan Spike protein trimer (SmT1v3)
225 adjuvanted with a proteasome-based intranasal adjuvant BDx301¹⁹⁻²¹. We have demonstrated that NT-
226 CoV2-1 induces superior mucosal and comparable systemic immune responses to aluminum phosphate-
227 adjuvanted formulations in mice and is able to suppress SARS-CoV-2 infection in hamsters. Unlike vector-
228 based intranasal vaccine candidates³⁹, protein subunit vaccines such as NT-CoV2-1 can be enhanced with
229 the addition of an adjuvant and avoid the potential inhibition due to anti-vector antibodies induced by
230 prior administration of the same vector. These results support further development of the NT-CoV2-1
231 vaccine.

232 **Materials and Methods:**

233

234 *Animals and Virus*

235 Female BALB/c mice (8-12 weeks old) and both male and female golden Syrian hamsters (81-90 g) were
236 obtained from Charles River Laboratories (Saint-Constant, Canada). Animals were maintained at the small
237 animal facility of the National Research Council Canada (NRC) in accordance with the guidelines of the
238 Canadian Council on Animal Care. All procedures performed on animals in this study were in accordance
239 with regulations and guidelines reviewed and approved in animal use protocol 2020.06 & 2020.10 by the
240 NRC Human Health Therapeutics Animal Care Committee.

241 The ancestral reference strain of SARS-CoV-2 (isolate Canada/ON/VIDO-01/2020 obtained from the
242 National Microbiology Lab, Winnipeg, Canada) was propagated and quantified on Vero E6 cells. Whole
243 viral genome sequencing was carried out to confirm exact genetic identity to original isolate. Passage 3
244 virus stocks were used in all subsequent experiments.

245

246 *Vaccine antigen and adjuvants*

247 Recombinant SmT1v3 Spike trimer constructs are based on “tagless” versions of the SARS-CoV-2 Spike
248 trimers described previously^{40,41}. Briefly, the SARS-CoV-2 reference strain Spike ectodomain sequence
249 (amino acids 1-1208 derived from Genbank accession number MN908947) was codon-optimized for
250 Chinese Hamster Ovary (CHO) cells and synthesized by GenScript (Piscataway, NJ, USA). Within the
251 construct, the Spike glycoprotein was preceded by its natural N-terminal signal peptide and fused at the
252 C-terminus to human resistin (accession number NP_001180303.1, amino acids 23-108). Mutations were
253 added to stabilize the generated Spike protein as previously described; amino acids 682-685 (RRAR) and
254 986-987 (KV) were replaced with GGAS and PP, respectively^{42,43}. Constructs were then cloned into the
255 pTT241 plasmid that did not encode C-terminal FLAG/His affinity tags. Expression constructs for VOC Spike
256 variants were prepared by re-synthesizing and replacing restriction fragments encompassing mutations
257 present in the Beta (SmT1v3-B) (D80A, D215G, 241del, 242del, 243del, K417N, E484K, N501Y, D614G,
258 A701V) and Delta (SmT1v3-D) (T19R, G142D, E156-, F157-, R158G, L452R, T478K, D614G, P681R, D950N)
259 variants, while maintaining the codon-optimized sequences of the remaining amino acids used for
260 SmT1v3-Reference (R) expression. Stably transfected pools were established by methionine sulfoximine
261 selection using the CHO²³⁵³ cell line and used for 10-day fed-batch productions with cumate induction as
262 described⁴¹. SmT1v3-R and -D were purified using a one-step affinity method with NGL COVID-19 Spike

263 Protein Affinity Resin (Repligen, Waltham, MA, USA). 150-250 ml of supernatant was applied to a 15-ml
264 column by gravity flow; Dulbecco's Phosphate Buffered Saline (DPBS) was used for column equilibration
265 and wash steps while the elution buffer consisted of 100 mM sodium acetate, pH 3.5. SmT1v3-B was
266 purified using a proprietary multi-step non-affinity-based process. After purification, proteins were
267 formulated by buffer exchange (using P100 desalting columns (CentriPure, EMP Biotech, Berlin,
268 Germany)) or tangential flow filtration (Minimate 30K cassettes (Pall, Port Washington, NY, USA)) in DPBS
269 adjusted to pH 7.8 at protein concentrations of 0.9-1.1 mg/ml. Purified proteins analyzed by sodium
270 dodecyl sulfate-polyacrylamide gel electrophoresis (SDS-PAGE) and analytical size-exclusion ultra-high
271 performance liquid chromatography (SEC-UPLC). SEC-UPLC was run on an Acquity H-Class Bio UPLC system
272 (Wyatt Technology, Santa Barbara, CA, USA) in phosphate buffered saline (PBS) + 0.02% Tween-20 on a
273 4.6 × 300 mm Acquity BEH450 column (2.5 µm bead size; Waters Limited, Mississauga, ON, Canada)
274 coupled to a miniDAWN Multi-Angle Light Scattering (MALS) detector and Optilab T-rEX refractometer
275 (Wyatt Technology). The identity and purity of the antigens was also confirmed by mass spectrometry.
276 Absence of endotoxin contamination was verified using Endosafe cartridge-based Limulus amoebocyte
277 lysate tests (Charles River Laboratories, Charleston, SC, USA).

278 BDX301 was prepared from cultures of *Neisseria meningitidis* by detergent extraction and ethanol
279 precipitation as described previously⁴⁴. AdjuPhos™ (Invivogen, SanDiego, CA, USA) was prepared as per
280 manufacturer's instructions.

281

282 *Immunization and sample collection*

283 Antigen and adjuvant vaccine components were diluted in DPBS (Cytiva, Marlborough, Massachusetts,
284 USA) and then admixed in glass vials (Thermo Fisher Scientific) prior to administration. Antigen and
285 adjuvant doses were chosen based on findings from previous studies. Mice were first anesthetized with
286 isoflurane then immunized by intramuscular injection (100 µL split equally into the left and right tibialis
287 anterior muscles) or by intranasal administration (10 µL per nare) on Days 0 and 21. Blood was collected
288 from isoflurane-anesthetized mice, via the submandibular vein on Days 21 (prior to boost) and 35. All
289 mice were humanely euthanized on Day 35 to collect bronchoalveolar lavage (BAL) fluid. Hamsters were
290 first anesthetized with 3-5% isoflurane and then immunized by intramuscular injection (100 µL) into the
291 left tibialis anterior muscle or by intranasal administration (20 µL per nare) on Days 0 and 21. Blood was
292 collected from isoflurane-anesthetized hamsters, via the anterior vena cava on Days 20 and 35. On Day
293 42, all Hamsters were anesthetized by intraperitoneal injection with 100 mg/kg of ketamine and 7 mg/kg

294 of xylazine prior to an intranasal challenge with 1×10^5 PFU of SARS-CoV-2. Hamsters were monitored
295 daily for body weight change and clinical signs. On Day 47, hamsters were euthanized and nasal turbinate
296 and the left lung were collected for assessment of viral load by plaque assay as described below.

297

298 *Anti-Spike IgG ELISA*

299 Anti-Spike total IgG titers in serum were quantified by ELISA. Briefly, 96-well high-binding ELISA plates
300 (Thermo Fisher Scientific) were coated overnight at room temperature (RT) with 100 μ L of 0.3 μ g/mL Spike
301 protein (same as used for immunization) diluted in PBS. Plates were washed five times with PBS/0.05%
302 Tween20 (PBS-T; Sigma-Aldrich, St. Louis, MO, USA), and then blocked for 1 hour at 37 °C with 200 μ L 10%
303 fetal bovine serum (FBS; Thermo Fisher Scientific) in PBS. After the plates were washed five times with
304 PBS-T, 3.162-fold serially diluted samples in PBS-T with 10% FBS were added in 100 μ L volumes and
305 incubated for 1 hour at 37 °C. After five washes with PBS-T (Sigma-Aldrich), 100 μ L of goat anti-mouse IgG
306 -HRP (1:4,000, Southern Biotech, Birmingham, AL, USA) or goat anti-hamster IgG-HRP (1:32,000, Southern
307 Biotech) was added for 1 hour at 37 °C. After five washes with PBS-T, 100 μ L/well of the substrate o-
308 phenylenediamine dihydrochloride (OPD, Sigma-Aldrich) diluted in 0.05 M citrate buffer (pH 5.0) was
309 added. Plates were developed for 30 minutes at RT in the dark. The reaction was stopped with 50 μ L/well
310 of 4N H₂SO₄. Bound IgG Abs were detected spectrophotometrically at 450 nm. Titers for IgG in serum
311 were defined as the dilution that resulted in an absorbance value (OD 450) of 0.2 and were calculated
312 using XLfit software (ID Business Solutions, Guildford, UK). Samples that do not reach the target OD were
313 assigned the value of the lowest tested dilution (i.e. 10) for analysis purposes.

314

315 *Anti-Spike IgA ELISA*

316 Anti-Spike IgA titers were also measured by indirect ELISA. Specifically, 96-well high-binding ELISA plates
317 (Thermo Fisher Scientific) were coated overnight at 4 °C with 100 μ L of 0.8 μ g/mL (80 ng/well) of Spike
318 protein diluted in PBS. After washing plates with PBST, wells were blocked with 200 μ L 3% Skim milk
319 (Thermo Fisher Scientific) in PBS and incubated at 37 °C for 2 hours and washed with PBST. 100 μ L of
320 sample was loaded on the plates using half-log serial dilution (equivalent to 3.162 x serial dilution starting
321 at 1:10) and incubated at 37 °C for 1 hour. Plates were washed again with PBST and 100 μ L of goat anti-
322 mouse IgA-HRP (Abcam, Cambridge, UK) diluted 1:10,000 added to each well. Plates were incubated at
323 37 °C for 45 min and washed with PBST. 100 μ L of TMB substrate Sure-blue reserve one-component
324 (Mandel Scientific Company Inc., Guelph, ON, Canada) was then added to each well and reaction stopped

325 after 10 min incubation at room temperature by adding 100 μ L of TMB stop solution one-component
326 (Mandel Scientific Company Inc., Guelph, ON, Canada). Bound IgA Abs were detected
327 spectrophotometrically at 450 nm, and IgA antibody titers were determined as above for IgG.

328

329 *Vero E6 Cell-based Surrogate SARS-CoV-2 Neutralization Assay*

330 This surrogate neutralization assay was performed similarly to conventional pseudoparticle neutralization
331 assays⁴⁵. Briefly, the ability of labeled SARS-CoV-2 Spike trimers to bind the surface of Vero E6 cells
332 following co-incubation with sera/plasma was measured. Vero E6 cells were maintained in RPMI 1640
333 supplemented with 10% FBS, 1% penicillin/streptomycin, 20mM HEPES, 1x non-essential amino acids, 1x
334 Glutamax, 50 μ M 2-mercaptoethanol (all from Thermo Fisher Scientific) at 37°C with 5% CO₂. Soluble
335 SmT1v3, was biotinylated and isolated from free biotin using EZ-Link™ NHS-LC-LC-Biotin (Thermo Fisher
336 Scientific) according to manufacturer's instructions. Indicated dilutions of mouse/hamster serum were
337 incubated with 250 ng of biotinylated Spike and 1x10⁵ Vero E6 cells (ATCC® CRL-1586™) in the presence
338 of PBS, 0.05% sodium azide (Thermo Fisher Scientific) and 1% bovine serum albumin (BSA; Rockland,
339 Philadelphia, PA, USA) within a 96-well V-bottom plate (Nunc™, Thermo Fisher Scientific) for 1 hour at 4
340 °C, while protected from light. Regardless of serum concentration, the final volume of all samples was
341 normalized to 150 μ L. Cells were washed with PBS + 0.05% sodium azide + 1% BSA and incubated with
342 Streptavidin-phycoerythrin conjugate (Thermo Fisher Scientific) for 1 hour at 4 °C. After another wash,
343 the cells were fixed using CytoFix™ (Becton Dickinson, Franklin Lakes, NJ, USA) and resuspended in wash
344 buffer + 5mM EDTA for acquisition on an LSR Fortessa™ (Becton Dickinson). Percent neutralization was
345 calculated using the Geometric Mean Fluorescence Intensity (MFI) of PE (on singlet cell population) using
346 FlowJo™ 10 analysis software (Becton Dickinson) as shown in the following formula: % neutralization =
347 $100 - (100 \times (\text{Geometric MFI for PE of test sample} - \text{Geometric MFI for PE of negative control sample (i.e.}$
348 $\text{cells incubated only with Streptavidin-PE and without Spike protein})) / (\text{Geometric MFI for PE of positive}$
349 $\text{control sample (i.e., cells incubated with Spike without serum/plasma)} - \text{Geometric MFI for PE of negative}$
350 $\text{control sample}))$. For analysis purposes, samples with calculated values ≤ 0 were assigned a value of 0.

351

352 *Plaque Assay*

353 This assay was performed exclusively within a containment level 3 facility (CL3). Whole lung from each
354 hamster was homogenized in 1 mL PBS. The samples were centrifuged and the clarified supernatants were
355 used in a plaque assay. The plaque assay, in brief, was carried out by diluting the clarified lung homogenate
356 in a 1 in 10 serial dilution in infection media (1x DMEM, high glucose media supplemented with 1x non-

357 essential amino acid, 100 U/mL penicillin-streptomycin, 1 mM sodium pyruvate, and 0.1% bovine serum
358 albumin). Vero E6 cells were infected for 1 h at 37°C before the inoculum was removed and overlay media
359 was added, which consisted of infection media with 0.6% ultrapure, low-melting point agarose. The cells
360 were incubated at 37°C/5% CO₂ for 72 h. After incubation, cells were fixed with 10% formaldehyde and
361 stained with crystal violet. Plaques were enumerated and PFU was determined per gram of lung tissue.

362

363 *Plaque reduction neutralization tests (PRNT)*

364 All steps carried out for the PRNT assay was performed in a CL3 facility. Serum samples were inactivated
365 at 56°C for 30 min and stored on ice. A 1-in-2 serial dilution was carried out using inactivated serum.
366 Diluted serum was incubated with equal volume containing 100 PFU of SARS-CoV-2 at 37°C for 1 h,
367 followed by infection of Vero E6 cells. Adsorption of virus were carried out for 1 h at 37°C. Inoculum was
368 removed after adsorption and overlay media as described above was added over the infected cells. The
369 assay was incubated at 37°C/5% CO₂ for 72 h. After incubation, cells were fixed with 10% formaldehyde
370 and stained with crystal violet. Controls included naïve animal serum, as well as a no serum, virus-only
371 back-titer control. PRNT₈₀ is defined as the highest dilution of serum that results in 80% reduction of
372 plaque-forming units. Samples that did not result in an 80% reduction in PFUs were assigned the value of
373 the lowest tested dilution (i.e. 40) for analysis purposes.

374

375 *Statistical analysis*

376 Data were analyzed using GraphPad Prism® version 9 (GraphPad Software, San Diego, CA, USA). Statistical
377 significance of the difference between groups was calculated by one-way or two-way analysis of variance
378 (ANOVA) followed by post-hoc analysis using Tukey's (comparison across all groups) multiple comparison
379 test. A Student's t-test was applied when analyzing the significance of the difference between the antigen-
380 specific IgG/IgA ratios in the BAL and serum. Data was log transformed (except for % neutralization,
381 IgG/IgA ratio and % body weight loss) prior to statistical analysis. For all analyses, differences were
382 considered to be not significant with $p > 0.05$. Significance was indicated in the graphs as follows: * $p <$
383 0.05 , ** $p < 0.01$, *** $p < 0.001$ and **** $p < 0.0001$.

384 **References**

- 385 1. Davis, C. *et al.* Reduced neutralisation of the Delta (B.1.617.2) SARS-CoV-2 variant of concern
386 following vaccination. *PLoS Pathog.* **17**, e1010022 (2021).
- 387 2. Pegu, A. *et al.* Durability of mRNA-1273 vaccine-induced antibodies against SARS-CoV-2 variants.
388 *Science* **373**, 1372–1377 (2021).
- 389 3. Tatsi, E.-B., Filippatos, F. & Michos, A. SARS-CoV-2 variants and effectiveness of vaccines: a review of
390 current evidence. *Epidemiol. Infect.* **149**, e237 (2021).
- 391 4. Baden, L. R. *et al.* Efficacy and Safety of the mRNA-1273 SARS-CoV-2 Vaccine. *N. Engl. J. Med.* **384**,
392 403–416 (2021).
- 393 5. Walsh, E. E. *et al.* Safety and Immunogenicity of Two RNA-Based Covid-19 Vaccine Candidates. *N.*
394 *Engl. J. Med.* **383**, 2439–2450 (2020).
- 395 6. Folegatti, P. M. *et al.* Safety and immunogenicity of the ChAdOx1 nCoV-19 vaccine against SARS-CoV-
396 2: a preliminary report of a phase 1/2, single-blind, randomised controlled trial. *The Lancet* **396**, 467–
397 478 (2020).
- 398 7. Castells, M. C. & Phillips, E. J. Maintaining Safety with SARS-CoV-2 Vaccines. *N. Engl. J. Med.* **384**, 643–
399 649 (2021).
- 400 8. Hatziantoniou, S., Maltezou, H. C., Tsakris, A., Poland, G. A. & Anastassopoulou, C. Anaphylactic
401 reactions to mRNA COVID-19 vaccines: A call for further study. *Vaccine* **39**, 2605–2607 (2021).
- 402 9. Greinacher, A. *et al.* Thrombotic Thrombocytopenia after ChAdOx1 nCov-19 Vaccination. *N. Engl. J.*
403 *Med.* **384**, 2092–2101 (2021).
- 404 10. Hayawi, K., Shahriar, S., Serhani, M. A., Alashwal, H. & Masud, M. M. Vaccine versus Variants
405 (3Vs): Are the COVID-19 Vaccines Effective against the Variants? A Systematic Review. *Vaccines* **9**,
406 1305 (2021).

- 407 11. Hou, Y. J. *et al.* SARS-CoV-2 Reverse Genetics Reveals a Variable Infection Gradient in the
408 Respiratory Tract. *Cell* **182**, 429-446.e14 (2020).
- 409 12. Holmgren, J. & Czerkinsky, C. Mucosal immunity and vaccines. *Nat. Med.* **11**, S45–S53 (2005).
- 410 13. Bilsborough, J. & Viney, J. L. Gastrointestinal dendritic cells play a role in immunity, tolerance,
411 and disease. *Gastroenterology* **127**, 300–309 (2004).
- 412 14. Burt, D. *et al.* Proteosome-adjuvanted intranasal influenza vaccines: advantages, progress and
413 future considerations. *Expert Rev. Vaccines* **10**, 365–375 (2011).
- 414 15. Fujikuyama, Y. *et al.* Novel vaccine development strategies for inducing mucosal immunity.
415 *Expert Rev. Vaccines* **11**, 367–379 (2012).
- 416 16. Rhee, J. H., Lee, S. E. & Kim, S. Y. Mucosal vaccine adjuvants update. *Clin. Exp. Vaccine Res.* **1**,
417 50–63 (2012).
- 418 17. Gupta, T. & Gupta, S. K. Potential adjuvants for the development of a SARS-CoV-2 vaccine based
419 on experimental results from similar coronaviruses. *Int. Immunopharmacol.* **86**, 106717 (2020).
- 420 18. Patel, G. B. & Chen, W. Archaeal lipid mucosal vaccine adjuvant and delivery system. *Expert Rev.*
421 *Vaccines* **9**, 431–440 (2010).
- 422 19. Mallett, C. P. *et al.* Intranasal or intragastric immunization with proteosome-Shigella
423 lipopolysaccharide vaccines protects against lethal pneumonia in a murine model of Shigella
424 infection. *Infect. Immun.* **63**, 2382–2386 (1995).
- 425 20. Orr, N., Robin, G., Cohen, D., Arnon, R. & Lowell, G. H. Immunogenicity and efficacy of oral or
426 intranasal Shigella flexneri 2a and Shigella sonnei proteosome-lipopolysaccharide vaccines in animal
427 models. *Infect. Immun.* **61**, 2390–2395 (1993).
- 428 21. Cao, W. *et al.* Nasal delivery of Protollin-adjuvanted H5N1 vaccine induces enhanced systemic as
429 well as mucosal immunity in mice. *Vaccine* **35**, 3318–3325 (2017).

- 430 22. Jones, T. *et al.* A nasal Proteosome™ influenza vaccine containing baculovirus-derived
431 hemagglutinin induces protective mucosal and systemic immunity. *Vaccine* **21**, 3706–3712 (2003).
- 432 23. Lambkin-Williams, R. *et al.* An Intranasal Proteosome-Adjuvanted Trivalent Influenza Vaccine Is
433 Safe, Immunogenic & Efficacious in the Human Viral Influenza Challenge Model. Serum IgG &
434 Mucosal IgA Are Important Correlates of Protection against Illness Associated with Infection. *PloS One*
435 **11**, e0163089 (2016).
- 436 24. Hu, M. C. *et al.* Intranasal Protollin-formulated recombinant SARS S-protein elicits respiratory
437 and serum neutralizing antibodies and protection in mice. *Vaccine* **25**, 6334–6340 (2007).
- 438 25. Akache, B. *et al.* Immunogenic and efficacious SARS-CoV-2 vaccine based on resistin-trimerized
439 spike antigen Smt1 and SLA archaeosome adjuvant. *Sci. Rep.* **11**, 21849 (2021).
- 440 26. Arunachalam, P. S. *et al.* Adjuvanting a subunit COVID-19 vaccine to induce protective immunity.
441 *Nature* **594**, 253–258 (2021).
- 442 27. Yilmaz, I. C. *et al.* Development and preclinical evaluation of virus-like particle vaccine against
443 COVID-19 infection. *Allergy* **77**, 258–270 (2022).
- 444 28. Akache, B., Stark, F. C., Agbayani, G., Renner, T. M. & McCluskie, M. J. Adjuvants: Engineering
445 Protective Immune Responses in Human and Veterinary Vaccines. *Methods Mol. Biol. Clifton NJ* **2412**,
446 179–231 (2022).
- 447 29. Bartsch, Y. C. *et al.* Discrete SARS-CoV-2 antibody titers track with functional humoral stability.
448 *Nat. Commun.* **12**, (2021).
- 449 30. Tada, T. *et al.* Convalescent-Phase Sera and Vaccine-Elicited Antibodies Largely Maintain
450 Neutralizing Titer against Global SARS-CoV-2 Variant Spikes. *mBio* **12**, e0069621 (2021).
- 451 31. Imai, M. *et al.* Syrian hamsters as a small animal model for SARS-CoV-2 infection and
452 countermeasure development. *Proc. Natl. Acad. Sci.* **117**, 16587–16595 (2020).

- 453 32. Ella, R. *et al.* Efficacy, safety, and lot to lot immunogenicity of an inactivated SARS-CoV-2 vaccine
454 (BBV152): a, double-blind, randomised, controlled phase 3 trial. *medRxiv* (2021).
- 455 33. King, R. G. *et al.* Single-Dose Intranasal Administration of AdCOVID Elicits Systemic and Mucosal
456 Immunity against SARS-CoV-2 and Fully Protects Mice from Lethal Challenge. *Vaccines* **9**, 881 (2021).
- 457 34. Cromer, D. *et al.* Neutralising antibody titres as predictors of protection against SARS-CoV-2
458 variants and the impact of boosting: a meta-analysis. *Lancet Microbe* **3**, e52–e61 (2022).
- 459 35. Riemersma, K. K. *et al.* Shedding of Infectious SARS-CoV-2 Despite Vaccination. *medRxiv* (2021).
- 460 36. Langel, S. N. *et al.* Oral and intranasal Ad5 SARS-CoV-2 vaccines decrease disease and viral
461 transmission in a golden hamster model. *BioRxiv* (2021).
- 462 37. van Doremalen, N. *et al.* Intranasal ChAdOx1 nCoV-19/AZD1222 vaccination reduces viral
463 shedding after SARS-CoV-2 D614G challenge in preclinical models. *Sci. Transl. Med.* **13**, eabh0755
464 (2021).
- 465 38. Lund, F. E. & Randall, T. D. Scent of a vaccine. *Science* **373**, 397–399 (2021).
- 466 39. Tioni, M. F. *et al.* One mucosal administration of a live attenuated recombinant COVID-19
467 vaccine protects nonhuman primates from SARS-CoV-2. 2021.07.16.452733 (2021).
- 468 40. Stuiblé, M. *et al.* Optimization of a high-cell-density polyethylenimine transfection method for
469 rapid protein production in CHO-EBNA1 cells. *J. Biotechnol.* **281**, 39–47 (2018).
- 470 41. Isho, B. *et al.* Persistence of serum and saliva antibody responses to SARS-CoV-2 spike antigens
471 in COVID-19 patients. *Sci. Immunol.* **5**, (2020).
- 472 42. Wrapp, D. *et al.* Cryo-EM structure of the 2019-nCoV spike in the prefusion conformation.
473 *Science* **367**, 1260–1263 (2020).
- 474 43. Pallesen, J. *et al.* Immunogenicity and structures of a rationally designed prefusion MERS-CoV
475 spike antigen. *Proc. Natl. Acad. Sci. U. S. A.* **114**, E7348–E7357 (2017).

- 476 44. US Patent for Compositions and methods for activating innate and allergic immunity Patent
477 (Patent # 9,433,672 issued September 6, 2016) - Justia Patents Search.
478 <https://patents.justia.com/patent/9433672>.
- 479 45. Wrapp, D. *et al.* Structural Basis for Potent Neutralization of Betacoronaviruses by Single-
480 Domain Camelid Antibodies. *Cell* **181**, 1004-1015.e15 (2020).
481

482 **Author Contributions:** FCS, BA, CDZ, TRC and MH conceived and designed the studies. LD, MS, YD, GA,
483 TMR, RD, BAH, DD, JB, SM, JZ, and MG contributed to the synthesis of the vaccine components and/or
484 execution of the experiments. FCS, BA, LD, AT, GA, TMR, RD, BAH, DD, JB, SRM and CDZ analyzed the data.
485 FCS, BA, JZ and CDZ took the lead in writing the manuscript. All authors provided critical feedback and
486 helped to shape the research, data analysis and manuscript.

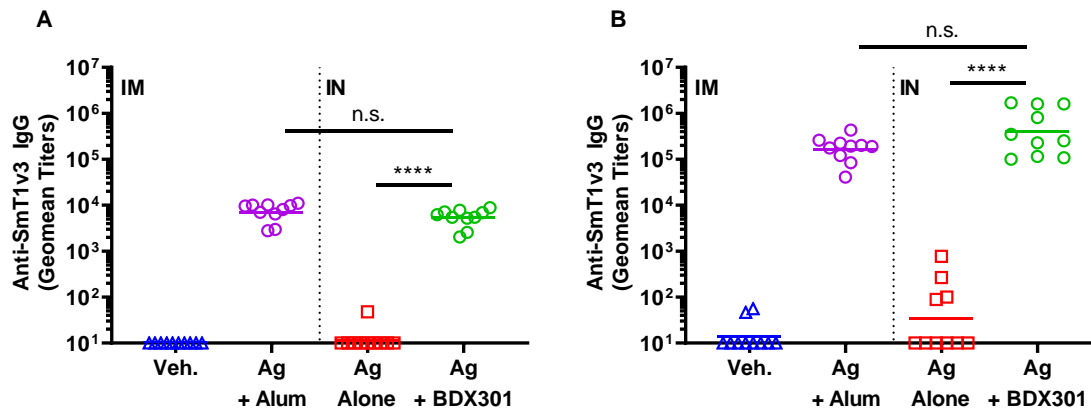
487 **Funding:** This research was funded by Oragenics Inc.

488 **Institutional Review Board Statement:** Animals were maintained at the small animal facility of the
489 National Research Council (NRC) Canada in accordance with the guidelines of the Canadian Council on
490 Animal Care. All procedures performed on animals in this study were approved by our Institutional Review
491 Board (NRC Human Health Therapeutics Animal Care Committee) and covered under animal use protocols
492 2020.06 & 2020.10. All experiments were carried out in accordance with the ARRIVE guidelines.

493 **Data Availability Statement:** The data presented in this study are available on request from the
494 corresponding author. The data are not publicly available due to privacy concerns.

495 **Acknowledgments:** The authors would like to acknowledge the technical contribution of many members
496 of the Mammalian Cell expression Section and Animal Resources Group of the NRC-HHT.

497 **Competing Interests:** CDZ, TRC and MH declare a potential conflict of interest as per their
498 employment/contract relationships with Oragenics. CDZ owns Oragenics stock options, and MH owns
499 Oragenics stock and options. JZ declares a potential conflict of interest as a shareholder in Inspirevax who
500 own commercial rights to BDX301.



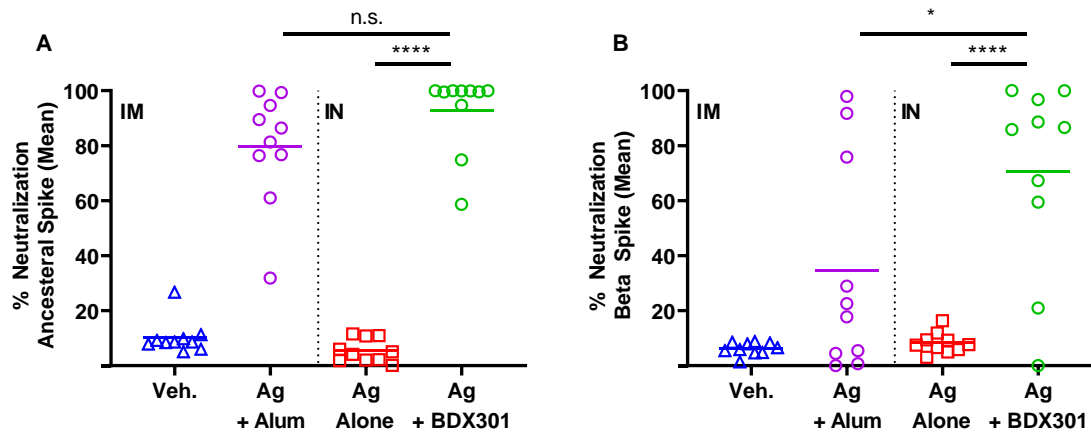
501

502

503 **Figure 1:** Anti-Spike IgG titers induced by SmT1v3 and BDX301 formulations in mice. BALB/c mice
504 (n=10/group) were immunized twice on Days 0 and 21. Vehicle control (Veh.) or the antigen (Ag) SmT1v3
505 (10 µg) with aluminum phosphate (Alum) (100 µg) were administered via the intramuscular (IM) route,
506 while SmT1v3 (10 µg) with or without BDX301 (5 µg) were administered via the intranasal (IN) route.
507 Serum collected 21 days after the 1st dose (Panel A) and 14 days after the 2nd dose (Panel B) were analyzed
508 by ELISA to determine the levels of antigen-specific IgG titers. Antibody titers are expressed as a reciprocal
509 value of the serum dilution calculated to generate an OD450 = 0.2. For statistical analysis, antibody titers
510 were log-transformed and then analyzed by a one-way ANOVA with Tukey's multiple comparisons test.
511 ****: p<0.0001, n.s.: no significant difference.

512

513



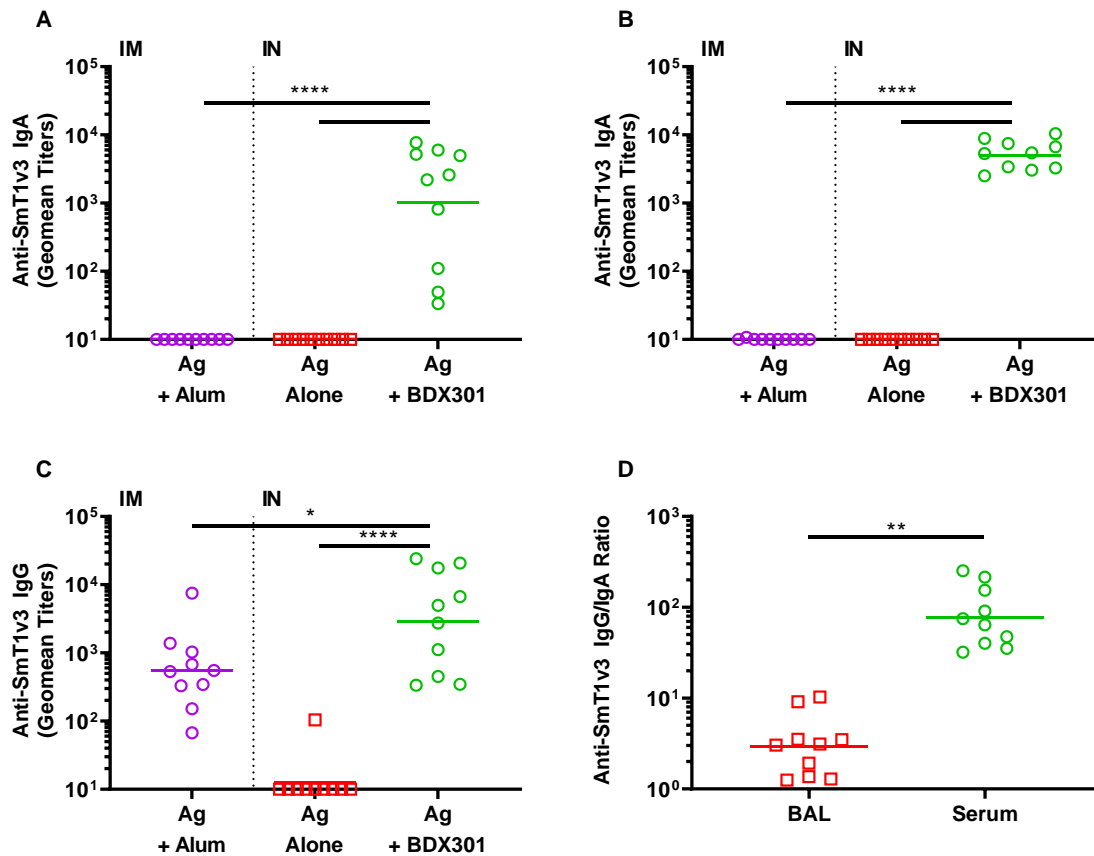
514

515

516 **Figure 2:** Neutralization activity induced by SmT1v3 and BDx301 vaccine formulations in mice. BALB/c
517 mice (n=10/group) were immunized twice on Days 0 and 21 with PBS (vehicle control, Veh.) or the antigen
518 (Ag) SmT1v3 (10 µg), with or without aluminum phosphate (Alum) (100 µg), via the intramuscular (IM)
519 route or SmT1v3 (10 µg), with or without BDx301 (5 µg), via the intranasal (IN) route. Serum collected on
520 Day 35 was diluted 75-fold and analyzed for its ability to block binding of Spike protein based on the
521 ancestral reference strain (Panel A) or Beta variant (Panel B) to VERO E6 cells. The neutralization activity
522 is calculated as a percent reduction from signal seen with control cells incubated in the absence of serum.
523 For statistical analysis, values were analyzed by a one-way ANOVA with Tukey's multiple comparisons test.
524 ****: p<0.0001, *:p<0.05, n.s.: no significant difference.

525

526

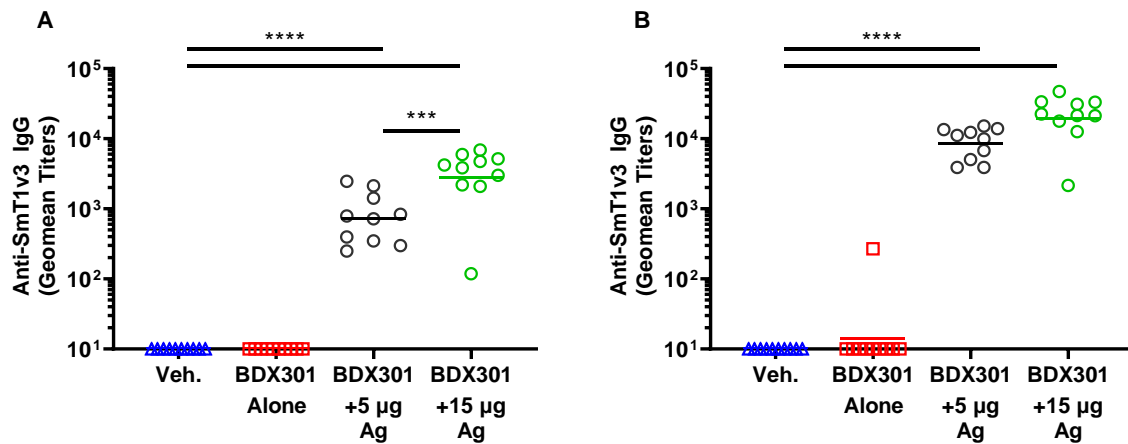


527

528 **Figure 3:** Comparison of anti-Spike IgA and IgG titers induced by SmT1v3 and BDX301 formulations in
529 serum and lungs of mice. BALB/c mice (n=10/group) were immunized twice on Days 0 and 21. The antigen
530 (Ag) SmT1v3 (10 µg) with aluminum phosphate (Alum) (100 µg) was administered via the intramuscular
531 (IM) route, while SmT1v3 (10 µg), with or without BDX301 (5 µg), were administered via the intranasal
532 (IN) route. Bronchoalveolar lavage (BAL; Panel A) or serum (Panel B) collected on Day 35 were analyzed
533 by ELISA to determine the levels of antigen-specific IgA titers. Levels of antigen-specific IgG titers were
534 also measured in the BAL (Panel C) and used along with serum IgG titers from Figure 1B to determine the
535 anti-SmT1v3 IgG/IgA ratios in both BAL and serum for the Ag+BDX301-immunized mice (Panel D).
536 Antibody titers are expressed as a reciprocal value of the BAL or serum dilution calculated to generate an
537 OD₄₅₀ = 0.2. For statistical analysis, antibody titers were log-transformed and then analyzed by a one-
538 way ANOVA with Tukey's multiple comparisons test, while IgG/IgA ratios were analyzed by a Student's t-
539 test. ****: p<0.0001, **:p<0.01, *:p<0.05.

540

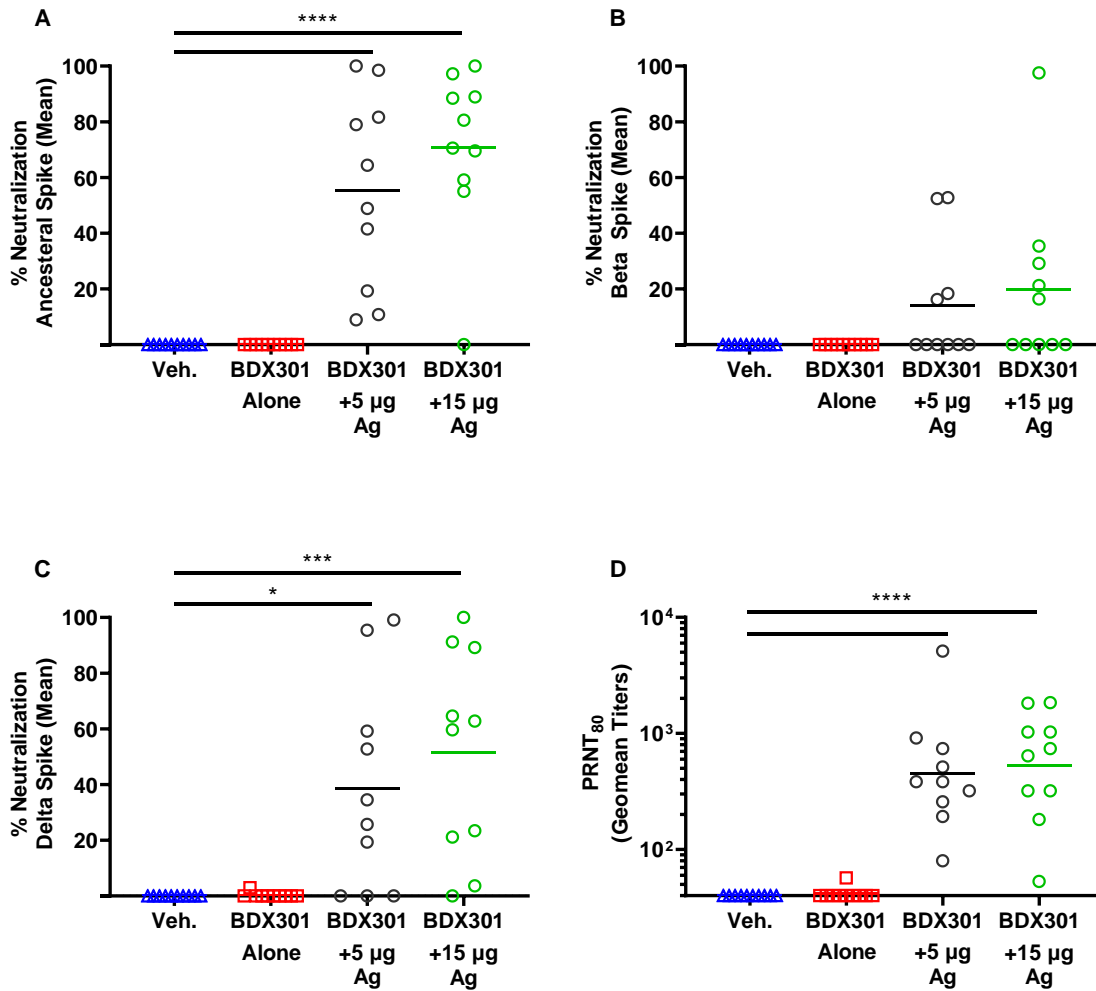
541



542
543 **Figure 4:** Anti-Spike IgG titers induced by SmT1v3 and BDX301 formulations in hamsters. Syrian Golden
544 hamsters (n=10/group) were immunized twice on Days 0 and 21 with PBS (vehicle control, Veh.) delivered
545 intramuscularly or BDX301 (5 µg) with or without SmT1v3 (5 µg or 15 µg) via the intranasal route. Serum
546 collected on Day 20 (Panel A) and Day 35 (Panel B) were analyzed by ELISA to determine the levels of
547 antigen-specific IgG titers. Antibody titers are expressed as a reciprocal value of the serum dilution
548 calculated to generate an OD₄₅₀ = 0.2. For statistical analysis, antibody titers were log-transformed and
549 then analyzed by a one-way ANOVA with Tukey's multiple comparisons test. ***: p<0.001, ****:
550 p<0.0001.

551

552

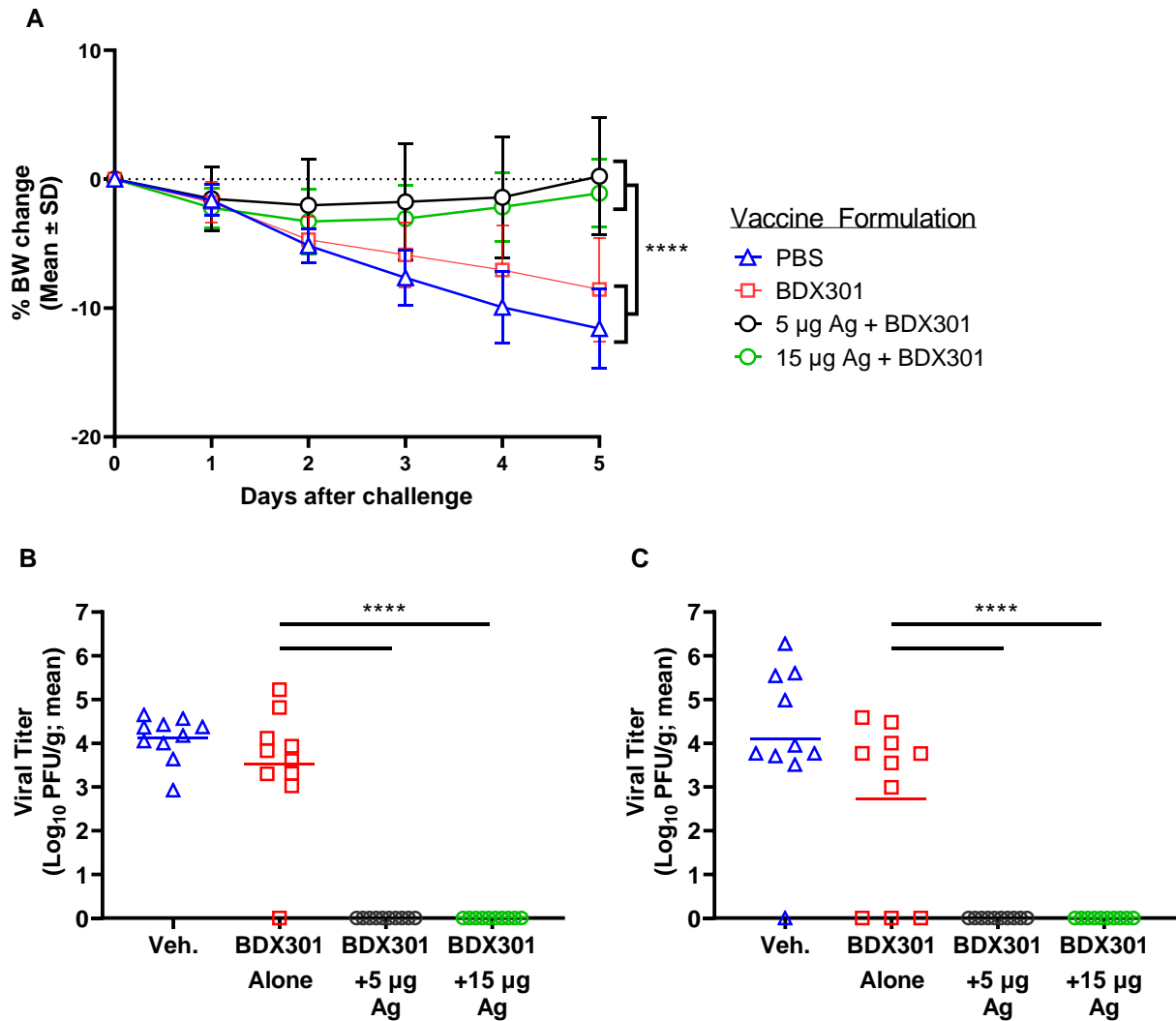


553

554

555 **Figure 5:** Neutralization activity induced by SmT1v3 and BDX301 formulations in hamsters. Syrian Golden
556 hamsters (n=10/group) were immunized twice on Days 0 and 21 with PBS (vehicle control, Veh.) delivered
557 intramuscularly or BDX301 (5 µg) with or without SmT1v3 (5 µg or 15 µg) via the intranasal route. Serum
558 collected on Day 35 was diluted 25-fold and analyzed for its ability to block binding of Spike protein based
559 on the ancestral reference strain (Panel A), Beta variant (Panel B) or Delta variant (Panel C) to VERO E6
560 cells. The neutralization activity is calculated as a percent reduction from signal seen with control cells
561 incubated in the absence of serum. Sera from Day 35 was also tested by a plaque reduction neutralization
562 test for its ability to block infection of VERO cells by SARS-CoV-2 (ancestral reference strain). PRNT titers
563 are expressed as a reciprocal value of the serum dilution calculated to generate an 80% reduction from
564 the number of plaques observed in control wells without serum. For statistical analysis, values were
565 analyzed by a one-way ANOVA with Tukey's multiple comparisons test. ****: p<0.0001, ***: p<0.001,
566 *:p<0.05, n.s.: no significant difference.

567



568
569 **Figure 6:** Efficacy of SmT1v3 and BDX301 formulations against SARS-CoV-2 viral challenge in hamsters.
570 Syrian Golden hamsters were immunized twice on Days 0 and 21 with PBS (vehicle control, Veh.) delivered
571 intramuscularly or BDX301 (5 µg) with or without SmT1v3 (5 or 15 µg) via the intranasal route. On Day 42
572 all hamsters were challenged with 1×10^5 PFU of SARS-CoV-2. Hamsters were monitored daily for body
573 weight change post-challenge (Panel A). On Day 47, hamsters were euthanized and viral titers were
574 quantified in lung (Panel B) and nasal turbinates (Panel C) by plaque assay. For statistical analysis, a two-
575 way (Panel A) or one-way (Panels B & C) ANOVA with Tukey's multiple comparisons test was performed.
576 ****: $p < 0.0001$, ***: $p < 0.001$.

577